Macromolecular Research, Vol. 25, No. 2, pp 97-107 (2017)
DOI 10.1007/s13233-017-5009-9

www.springer.com/13233
pISSN 1598-5032 eISSN 2092-7673

Feature Article

Surface-Initiated Polymerization with Poly(*n*-hexylisocyanate) to Covalently Functionalize Silica Nanoparticles

Fatma Vatansever*[,1,2] and Michael R. Hamblin*[,1,2,3]

[1]*Wellman Center for Photomedicine, Massachusetts General Hospital, Boston, MA 02114, USA*
[2]*Department of Dermatology, Harvard Medical School, Boston, MA 02115, USA*
[3]*Harvard-MIT Division of Health Sciences and Technology, Boston, MA 02139, USA*

Received September 2, 2015; Revised October 12, 2016; Accepted October 19, 2016

Abstract: New methods are needed for covalent functionalization of nanoparticles-surface with organic polymer coronas to generate polymeric nanocomposite in a controlled manner. Here we report the use of a surface-initiated polymerization approach, mediated by titanium(IV) catalysis, to grow poly(*n*-hexylisocyanate) chains from silica surface. Two pathways were used to generate the interfacing in these nano-hybrids. In the first one, the nanoparticles were "seeded" with $SiCl_4$, followed by reaction with 1,6-hexanediol to form hydroxyl groups attached directly to the surface *via* O-Si-O bonding. In the second pathway, the nanoparticles were initially exposed to a 9:1 mixture of trimethyl silyl chloride and chlorodimethyl octenyl silane which was then followed by hydroboration of the double bonds, to afford hydroxyl groups with a spatially controlled density and surface-attachment *via* O-Si-C bonding. These functionalized surfaces were then activated with the titanium tetrachloride catalyst. In our approach, surface tethered catalyst provided the sites for *n*-hexyl isocyanate monomer insertion to "build up" the surface-grown polymer layers from the "bottom-up". A final end-capping, to seal off the chain ends, was done *via* acetyl chloride. Compounds were characterized by Fourier transform infrared spectroscopy (FTIR), ^{1}H nuclear magnetic resonance spectroscopy (NMR), gas chromatography-mass spectrometry (GC-MS), gel permeation chromatography (GPC), and thermogravimetric analyses.

Keywords: polymeric nanocomposites, inorganic-organic interfacing, controlled polymerization, surface initiated polymerization, nanoparticle surface modification, titanium catalyst, *n*-hexyl isocyanate polymerization.

Introduction

With the expansion of interest in nanomaterials, nanotechnology, and nanocomposites in a wide range of applications and in various fields, such as energy transfer, optics,[1] optoelectronic devices,[2] and semiconductor devises, aerospace, medicine,[3] biotechnology,[4] biomedical science,[5,6] and textiles, nanoparticles (NP) surface modification became a prime research area. There is a pressing need to be able to tailor the surface of NP with desired functionality, density of functional groups, using a facile process amenable to scaling-up. This need is particularly important for hybrid inorganic-organic interfaces. The ability to attach organic layers or polymer coronas to inorganic (metallic, non-metallic, semiconductor) NP surfaces is of particular interest. Polymeric nanocomposites of inorganic nanoparticles with surface tethered polymer chains represent a "new class" of materials that offer a broad breath of application spectrum due to functional diversification.[7] Furthermore, polymers are good candidates for surface modification of NP due to their ability to form a flexible, multi-functionalized surface coverage with desired secondary properties.[8]

One of the drawbacks with many polymer-functionalization strategies of NP, however, is that the organic (polymer) layers are usually tethered to the inorganic surface by physical adsorption (physisorption) which leads to unstable surfaces, since the polymer interaction with the inorganic-surface is relatively weak in nature. Desorption or displacement of the polymer from the NP in the presence of solvent or a low molecular weight compound can easily take place. Moreover, weak interactions between the polymer and the NP surface also lead to a thermally labile surface, with non-homogeneous

*Corresponding Authors. E-mails: vatansever.fatma@mgh.harvard.edu or hamblin@helix.mgh.harvard.edu

coverage taking place upon heating, leading to changes in the physical properties of the surface. Therefore, generating a stable polymeric-nanocomposite construct with covalent connection between the two interfaces is of critical importance.

Covalent tethering of the polymer to the NP surface however, may adversely affect the spatial density of the organic component. The spatial density obtained using covalent grafting of pre-formed polymer chains could be significantly lower than physisorption, due to kinetic reasons, once the surface is substantially covered; the incoming polymer chains have to diffuse against the concentration gradient in order to reach the surface. In contrast, the spatial density obtained when the polymer chains are directly grown onto the surface of the NP can be much greater.[9] The goal of controlled/desired spatial density can be achieved by using a bifunctional-coupling strategy that can generate unhindered density of covalent bonding with the NP surface while also functioning as initiating- "seeding"- sites for the polymerization reaction, and thus acting as an adhesive to join the dissimilar surfaces. This "surface initiated" polymerization approach, enabling the growth of polymer chains "from the surface up", is an attractive method to generate well-functionalized, high-density, hybrid organic-inorganic nanomaterials with stable-attachment of the polymer layer.

In this paper we describe the functionalization of silica NP *via* the surface-initiated polymerization reaction of *n*-hexyl isocyanate. In our approach, the polymerization reaction was initiated from surface tethered alcohol groups *via* titanium alkoxide that mediated the polymerization of isocyanate monomers. The polymer chain length and average molecular weight of the chains were analyzed after cleaving the attached polymer chains at their acid sensitive site. All the air stable products were fully characterized.

Experimental

Instrumentation. Thermogravimetric analysis (TGA) thermograms were collected with TA Instruments thermogravimetric analysis system at a temperature scan rate of 20 °C with a 20 mL/min nitrogen purge. Infrared (IR) spectra were collected using the Nicolet Magna 560 system having both TGS and MCT detectors. The solution IR samples were prepared in a dry-box filled with a nitrogen gas with a drop of analyte placed between two KBr pellets. Air-stable solid samples were finely ground with dried KBr powder and prepared as pellets. High resolution ^{1}H nuclear magnetic resonance spectroscopy (NMR) spectra were collected on a Bruker AF-500 NMR Spectrometer. Gel permeation chromatography (GPC) data were collected with a Waters 150-C ALC/GPC ultrastyragel system combined with ultraviolet and diffractive index detectors. The μ-Styrene HT columns have 10^5 and 10^3 Å pore size and ran the sample in tetrahydrofuran at 35 °C with a flow rate of 1 mL/min. Narrow molecular weight polystyrene standards were used for calibration. Gas chromatography-mass spectrometry (GC-MS) data were collected with Agilent 6890 (GC) and 5972A (MS) syringeless injection equipment housing a 10 meter × 0.18 mm ID column, GC Phase of MTX-1 × 0.4 microns and a modified SGE Pyrojector II where our samples were heated within the pyrolysis furnace up to 950 °C and the pyrolysis products were transferred directly into the injection port for separation by GC and identification by MS.

Reagents. Grade M-5-"fumed silica" with surface area of 200±50 m^2/g was procured from CAB-O-SIL®, Cabot Corporation USA. Prior to any further treatment it was heated at 160 °C and 10^{-1} torr for 48 h in order to remove all the physisorbed water present and breaking the agglomerate to three-dimensional 200 nm +/- 20 nm mean diameter clusters of NP with high purity and enormous surface area. Silicon tetrachloride, chloro-trimethylsilane and chlorodimethyl-octenyl-silane were purchased from Acros and used as received. Hexyl isocyanate was distilled over CaH_2. Titanium tetrachloride was distilled over copper turnings. Toluene, hexane, and tetrahydrofuran were refluxed and distilled over Na/benzoquinone. Dichloromethane was distilled and stored over 4 Å molecular sieves. All solvents and reagents were degassed prior to use. Hexanediol was recrystallized using water and dried for several days over high vacuum.

Reactions.

Silylation Reactions (1, 6): In the glove box, dried fumed silica (250 mg) was added to a round bottomed flask and $SiCl_4$ (15 mL) was added. The mixture was stirred with a glass rod to produce slurry. Excess silicon tetrachloride was removed overnight on high vacuum to afford product **1**. In a similar manner, dried fumed silica (250 mg) was treated with a mixture of trimethyl silyl chloride and chlorodimethyl octenyl silane (15 mL, in a molar ratio of 9:1) where the slurry produced was stirred with a glass rod and excess of silylating agents was removed overnight on high vacuum at 50 °C to yield product **6**. In these reactions, as it can be seen from Scheme II, the silylating agents were tethered to the silica surface-hydroxyl groups (Si-OH groups) *via* their Si-Cl end, forming stable chemical bonding. Since these reactions were carried under an inert atmosphere, hydrolysis of the silylating agents (which is an extremely fast process) as well as the favorable water physisorption processes were avoided.

IR (KBr): 3000, 2960, 2919, 2870, 2853, 1100, 846, 840, 472.

^{1}H NMR ($CDCl_3$, in ppm): 5.40 (3H, m); 1.97 (2H, d); 1.62-1.26 (12H, m); 0.95-0.62 (2H, m); 0.32-0.05 (3H, m) and GC-MS (m/e): 73, 75, 111, 112, 168.

Hydroboration Reaction (7): Silica NP with pendant vinyl groups, **6**, (340 mg) was added to a round bottom flask with tetrahydrofuran (THF) (8 mL). Diborane solution in THF (1 M, 4 mL) was added dropwise in 4×1 mL portions. The reaction mixture was allowed to stir for one hour, and then cooled to 0 °C. Methanol (3 mL) was added dropwise followed by 3 M NaOH (3 mL) and 30% H_2O_2 solution (3 mL), while maintaining the reaction temperature with an ice bath. Reaction was allowed to stir for another hour after which it was filtered and washed several times with methanol (MeOH)

(5×15 mL) and overnight drying under high vacuum yielded **7**.

IR (KBr): 3400, 3000, 1630, 1100, 840, 472.

^{1}H NMR ($CDCl_3$, in ppm): 1.49 (br s, 3H); 1.19 (br s, 12H); 0.82-0.79 (m, 2H).

GC-MS (m/e): 41, 45, 59, 75, 101, 115, 129, 130, 143, 157, 171, 185.

Coupling Reaction (2): In the glove box, the chlorosilane-activated silica (with effective Si-Cl_3 groups tethered to the silica surface *via* the hydroxyl groups on the surface), compound **1** (100 mg) was added to a round bottom flask and a saturated solution of 1,6-hexanediol in dioxane (10 mL) was added. The reaction mixture was allowed to stand for 12 h and then filtered through a sintered funnel. It was washed several times with dioxane (5×10 mL) followed by a single wash of dioxane (5 mL) containing triethylamine (0.1 mL). This was followed by two washes with dioxane (2×10 mL) followed by hexane (2×10 mL). Hydroxyl-coated silica, compound **2**, was dried for over 12 h on high vacuum at room temperature.

IR (KBr): 3428 (br), 2939, 1635, 1457, 1099 (br), 806 cm^{-1}.

^{1}H NMR ($CDCl_3$, in ppm): 3.57 (t, 2H), 1.55-1.49 (m, 3H), 1.33-1.27 (m, 2H), 1.18-1.04 (m, 6H).

GC-MS (m/e): 27, 29, 31, 42, 55, 57, 70, 82, 117 (M^+).

Attachment of the Transition Metal Catalyst (3 and 8): Hydroxyl-terminated silica NP, **2**, (100 mg) was added to a round bottomed flask in hexane (10 mL) and then cooled to 0 °C. Pre-cooled $TiCl_4$ (300 mg) was added dropwise maintaining the reaction temperature at 0 °C. The reaction mixture was then allowed to warm up to room temperature and allowed to stir for 12 h. Filtration, washing five times with hexane (5×10 mL) and drying afforded **3**, which was stored at -40 °C under nitrogen. Hydroxyl-terminated silica NP, **7**, (100 mg) was treated as described above with cold $TiCl_4$ (300 mg) at 0 °C and worked up to afford the silica bound catalyst **8**.

Polymerization of the Monolayer (4, 5, and 9): *n*-Hexyl isocyanate (1 mL) was added to stirred **3** (4 mg) in toluene (0.1 mL). The reaction mixture became viscous and turned orange indicating the initiation of polymerization. The reaction was allowed to proceed for 2 h and then CH_3COCl (0.1 mL) was added as an end-capping agent. Reaction mixture was dissolved in 9:1 (THF:MeOH), and filtered. The residue was re-precipitated in MeOH to give a white solid, **4**. In the same manner, *n*-hexyl isocyanate (1 mL) was added to stirred **3** (4 mg) in toluene (0.1 mL) and the polymerization reaction was allowed to proceed for 5 h after which CH_3COCl (0.1 mL) was added as an end-capping agent. Following the same work-up, the white solid, **5**, was obtained.

IR (KBr): 2929, 2858, 1699, 1463, 1346, 1244, 1178, 1092, 997 cm^{-1}.

^{1}H NMR ($CDCl_3$, in ppm): 3.9-3.4 (m, 2H), 1.7-1.42 (m, 2H) 1.40-1.10 (m, 6H), 0.98-0.86 (br, 3H) and GC-MS (m/e): 15, 27, 29, 39, 41, 56, 84, 99, 112, 126.

In a similar manner, *n*-hexyl isocyanate (1 mL) was added to **8** (4 mg) in toluene (0.1 mL). The reaction was allowed to stir for 4 h after which CH_3COCl (0.1 mL) was added as anend-capping agent (that also inactivates the catalyst). Final work-up (described in details above) yielded the compound **9**.

Cleavage of the Polymer from the Silica Surface: Compound **4**, **5**, or **9** (10 mg) was added to chloroform: acetone mixture (1:1, 10 mL) containing HCl (0.1 mL). The reaction was allowed to stir for 12 h, and then filtered. The filtrate was concentrated and dissolved in THF:MeOH (9:1) mixture and re-precipitated in MeOH yielding the respective polymers cleaved off the silica surface.

Results and Discussion

Functionalizing NP "from the bottom-up" involves "seeding" the surface with a polymerization initiator or catalyst that will continue to be available to grow the extending polymer chains in presence of the monomer(s). This approach provides a defined density of "effective polymerization-sites" and the surface bound catalyst (which polymerizes *via* an insertion mechanism) will not synthesize a non-bound polymer, *i.e*., no side- and/or parallel- reactions in the reaction medium. Key feature in this surface-initiated polymerization (SIP) surface modification technique is introducing a surface-bound organometallic catalyst that serves as a "handle" through which monomers can polymerize and the reactivity of the "active polymer end" can be altered by manipulating the characteristics of the metal-catalyst end-group such as, ligand sphere, oxidation state, stereochemistry, *etc*. In this study we used Ti(IV) centered $TiCl_4$ as a catalyst for a "controlled" SIP from the silica NP surface with significantly high grafting density. We were able to achieve high surface-density due to using small monomer molecules that are readily reaching the active initiation-sites with the active-catalyst, thus we circumvented the steric barrier problem of incoming polymer chains.[10,11] Interestingly, a substrate tethered $TiCl_4$ catalyst has a unique way of reacting with the *n*-isocyanate monomers where it is known to insert the *n*-isocyanate monomers one at a time into a metal-ligand bonding[12] with the general mechanism given in Scheme I. A major advantage of this *n*-hexyl isocyanate polymerization technique is that it circumvents the drawbacks of anionic polymerization that suffers spirotetramerization and cyclic tetramerization as side reactions. During polymerization each consecutive *n*-hexyl isocyanate monomer is inserting itself between the metallic center and the previously bound monomer[13,14] forming the polymer chain as shown, Scheme I.

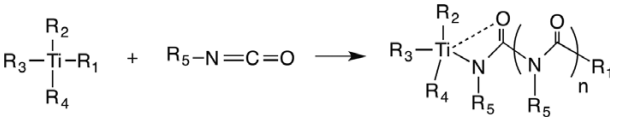

Scheme I. Formation of polymer chain growing on titanium catalyst.

Since $TiCl_4$ is an extremely electrophilic complex,[15] which readily reacts with alcohols at room temperature in an exothermic and extremely vigorous fashion, we have taken precautions to keep the reaction environment at 0 °C. To preserve the catalyst active throughout the polymerization processes we kept the reaction environment under dry nitrogen gas environment.

We have chosen to generate polymeric nanocomposites of *n*-hexyl isocyanate due to a unique dynamic structural modulation observed in the poly(*n*-hexyl isocyanate) chains. Poly(*n*-hexyl isocyanates) are shown to assume 8/3 helical structures[16,17] that are known to display lyotropic and thermotropic liquid crystallinity,[17-21] a property inherently significant for various functional applications.

In this paper we report two systems for obtaining terminal surface-bound hydroxyl end-functionalities: the first one is having a diol to react with a coupling agent treated silica surface and in the second one the alkene-terminated silica undergoes a hydroboration reaction to generate the desired terminal-hydroxyl groups. Interestingly, the second system used is actually a coupled hydroboration-oxidation reaction, where the borane (as a strong electrophile) adds to the double bond in a single step with boron adding to the less highly substituted carbon and hydrogen adding to the more highly substituted carbon (forming alkylborane). This orientation places the partial positive charge in the transition state on the more highly substituted carbon atom, since the electrophilic boron atom withdraws electrons from the pi bond, and the carbon at the other end of the double bond acquires a partially positive charge. This charge is more stable on more highly substituted carbon atom. The next step is the oxidation of the boron atom, removing it from the carbon and replacing with a hydroxyl group. With this anti-Markovnikov type addition, we were able to obtain surface bond hydroxyls with hydroxyl groups at the end of the chain. These terminal-hydroxyls groups were then used to tether the titanium catalyst to the NP surface to be used as "active" polymerization-sites.

We followed two distinct pathways in generating our surface modifications; described as Pathway I and II, as seen in Scheme II.

In order to grow polymer on the silica surface the surface needs to be carefully prepared. Amorphous silica, with its highly disordered surface-structure, is known to consist of interlinked SiO_4 tetrahedra comprising surface-terminal groups of both *siloxane* (Si-O-Si; with the oxygen on the surface) and *silanol* (Si-OH) groups.[22,23] Moreover, the silanols contain different types of hydroxyl groups: isolated silanols, vicinal (also known as bridged) silanols, and geminal silanols.[22,24-30] Thus, the silica surface is highly hydroxylated and these surface silanol groups are sites for further binding of water and/or other adsorbed molecules. In order to carry out our reactions, it was therefore necessary to remove all the physisorbed water (*i.e.* dehydration). However, preservation of the isolated hydroxyl groups, *i.e.* avoiding dehydroxylation, is of utmost importance in this functionalization. To ensure that we have preserved the isolated surface-OH groups at the end of the treatment, in addition to the standard Fourier transform infrared spectroscopy (FTIR), we carried out glass diffuse reflectance (GDR) and the diffuse reflectance infrared Fourier transform (DRIFT) studies as well. The presence of the NP'Si-OH groups was con-

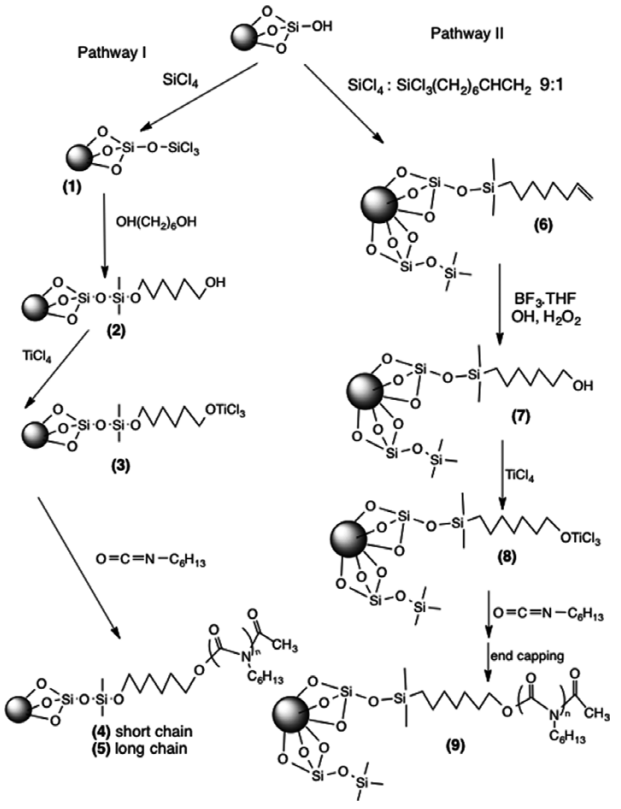

Scheme II. Synthetic reaction pathways I and II.

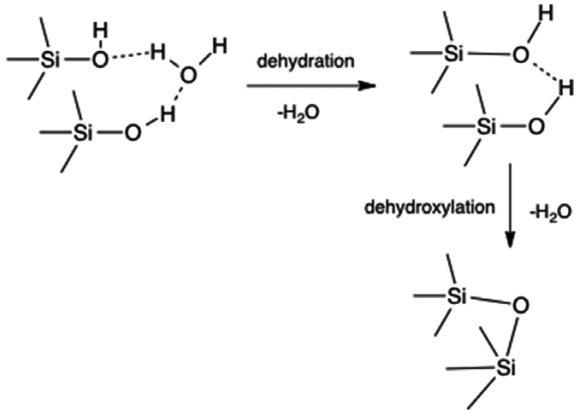

Scheme III. Removal of physisorbed water from silica surface. Removal of the physisorbed water unveils the silica surface with its siloxane, isolated hydroxyl, and hydrogen-bonded hydroxyl groups. Thus, the surface preparation process is of utmost importance where the surface hydroxyl groups ought to be preserved; over-drying can lead to excessive and undesired generation of siloxane groups at the expense of the hydroxyl groups; --- denotes hydrogen bonding.

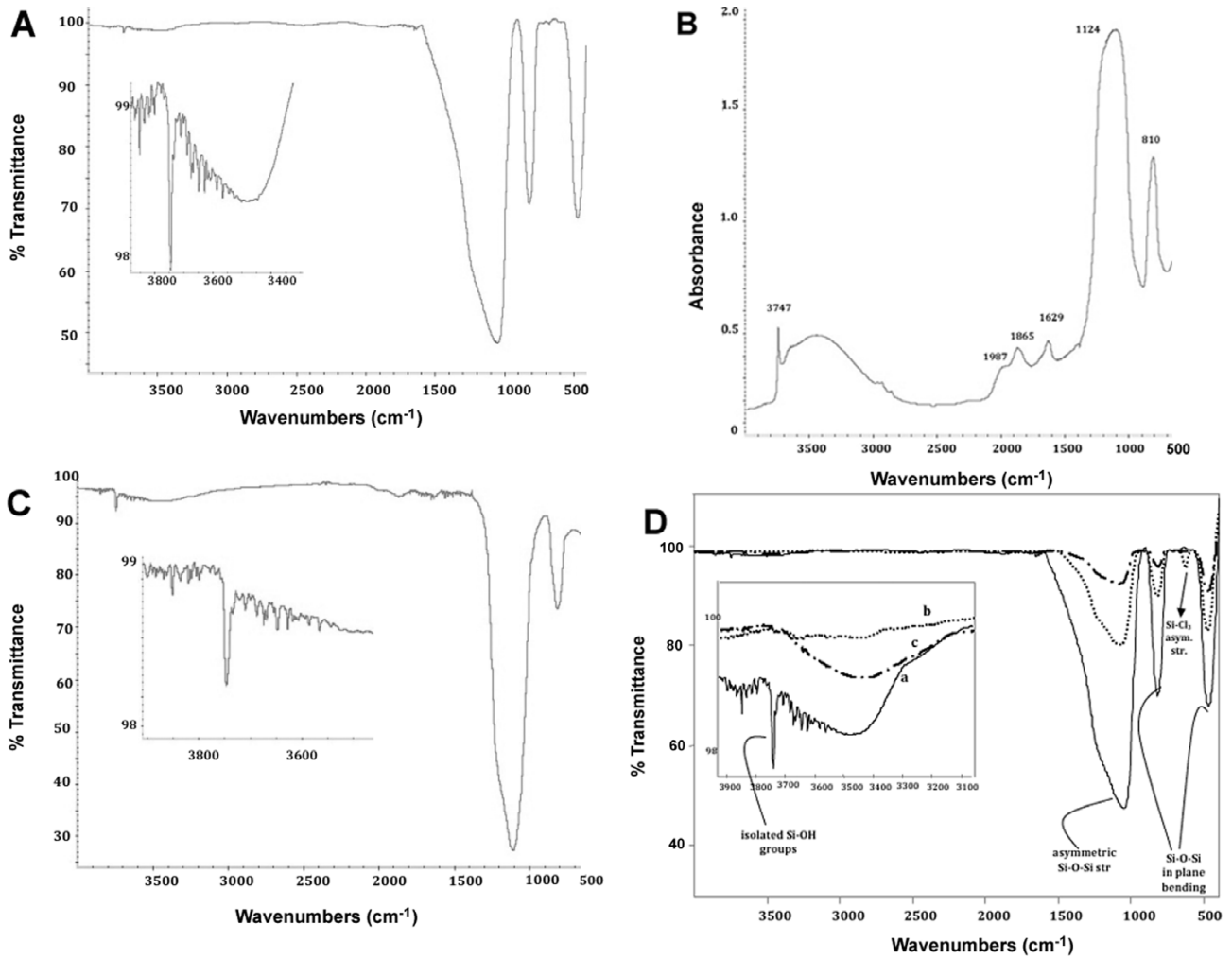

Figure 1. (A) FTIR spectrum of the dried silica; (B) GDR spectrum of the dried silica; (C) DRIFT spectrum of the dried silica; (D) Comparison of the FTIR spectra of (a) untreated-dried silica, (b) coupling agent covered silica (compound (**1**)), and (c) air-exposed silica (compound (**1**)).

firmed, as shown in Figure 1 and discussed in detail below.

It has been shown that heating nonporous silica at around 110 °C for a prolonged period removes the physisorbed water and at 225 °C the adjacent silanol groups start to condense and form water, Scheme III.

We heated our fumed silica substrate at 160 °C for 48 h in high-vacuum to obtain an almost completely dehydrated surface. The Fourier transform IR (FTIR) spectrum of the dried silica, Figure 1(A), has two main components; those pertaining to the surface hydroxyl groups and those due to the Si-O-Si backbone. The free isolated-hydroxyls can be seen at 3747 cm^{-1} with the free germinal-hydroxyls appearing at 3742 cm^{-1} where the hydrogen-bonding perturbed hydroxyls appear at the 3720-3730 cm^{-1} region. The other expected characteristic peaks related to the "silica backbone" indeed do appear as very strong absorption peaks and can be identified as: the asymmetric Si-O-Si stretching peak appearing at the 1110-1035 cm^{-1} region is centered at 1040 cm^{-1}; the Si-O-Si in-plane bending absorption peaks appear in two distinctive regions with 475-470 cm^{-1} and 820-820 cm^{-1} ranges.

In an effort to complement and enhance the FTIR information, we further conducted the "gold standard" characterization technique for silica, the Glass Diffuse Reflectance (GDR), in addition to Diffuse Reflectance Infrared Fourier Transform (DRIFT) studies.[31,32] The GDR spectrum (Figure 1(B)) provides more detailed information for the 3800-3500 cm^{-1} region with enhancement of the splitting pattern from the reflectance signal of the free isolated-hydroxyls at 3747 cm^{-1} and the free germinal-hydroxyls at 3742 cm^{-1} that are very characteristic for our silica substrate. Except for the reflectance from the hydrogen perturbed hydroxyls (at around 3722 to 3729 cm^{-1}), the rest of the features above 3600 cm^{-1} are artifacts caused by the water vapor in the chamber. The reflectance disturbance around 1990-1760 cm^{-1} is due to skeleton overtone vibrations in the silica network (as one will see in the discussion below, this feature is more pronounced in the

DRIFT spectrum). The other two features in the GDR spectrum of the fumed silica are due to Si-O-Si reflectance; the one at 1107 cm^{-1} is due to asymmetric stretching vibrations, and the one at 810 cm^{-1} is due to in plane bending vibrations. The DRIFT spectrum (Figure 1(C)) of the dried fumed silica confirms the skeleton overtone vibrations in the silica network, appearing at around 1987 cm^{-1} and at 1865 cm^{-1}. The free isolated-hydroxyls appear at around 3747 cm^{-1}. The Si-O-Si asymmetric stretching vibrations appear at 1112 cm^{-1} and the in plane bending at 810 cm^{-1}. We do not see the Si-O-Si stretching vibrations at 470-475 cm^{-1} region since both GDR and DRIFT use a mercury-cadmium-tellurite analyzer (MCTA) as a detector that has a cut-off at 650 cm^{-1}.

In pathway I dry fumed-silica was treated with silicon tetrachloride to form a monolayer of chlorosilane groups, Scheme II. It is important to carry this reaction in a glove-box under dry conditions as the presence of water will hydrolyze the chlorosilanes on the surface. As one can see from the FTIR results, Figure 1(D)(b) and (c), after treatment with $SiCl_4$, the peaks due to -$SiCl_3$ bonding appear at 625 cm^{-1} and are due to -Si-Cl asymmetric stretching absorption, while the symmetric stretching counterpart appears in the 535-450 cm^{-1} range; so the peak at 472 cm^{-1} is now due to absorptions from -$SiCl_3$ symmetric stretching and Si-O-Si stretching. To prove this point we exposed the IR pellet to air for 15 min and repeated the FTIR spectrum. The absorbance peak area before and after air exposure was measured, and, while that area was 18.50 for the unexposed sample, after exposure it decreased to 8.28. Moreover, the -$SiCl_3$ asymmetric stretching absorption peak disappeared, due to hydrolysis of $SiCl_3$ with air contact. These are clear indications that the peak at 472cm^{-1} is due to absorption from both Si-O-Si stretching and $SiCl_3$ symmetric stretching. As is seen from Figure 1(D)(b) and (c), the peak at 625 cm^{-1}, due to -$SiCl_3$ asymmetric stretching, disappears after air exposure. At the same time, a peak appears around 1625 cm^{-1}, as well as a broad peak above 3100 cm^{-1}. These last two peaks are due to water adsorption on (**1**) while the sample is exposed to air. The broad peak above 3100cm^{-1} is due to -OH stretching vibration's absorption, and the peak at 1625 cm^{-1} is due to -OH bending vibration absorption. Figure 1(D) shows the comparison of the FTIR spectra of untreated dry-silica (a) and coupling agent-reacted silica (compound (**1**)) (with unexposed one as (b) and air exposed and then IR re-taken one as (c). Clearly, in our dried silica, the IR absorption at 3747 cm^{-1} (due to the presence of free hydroxyl groups) disappears after the $SiCl_4$ coupling-reaction generates compound (**1**).

The product, compound (**1**), now has the appropriate functionality to form a chemical bond with our bifunctional coupling agent, the hexane diol. The hexane diol was recrystallized prior to use, using water. It was therefore dried for several days under high vacuum to get rid of all water. The saturated solution of hexane diol in dioxane was added to (**1**) at room temperature under inert conditions in the glove-box and left to stir for ~12 h. Filtration, washing the residue several times to

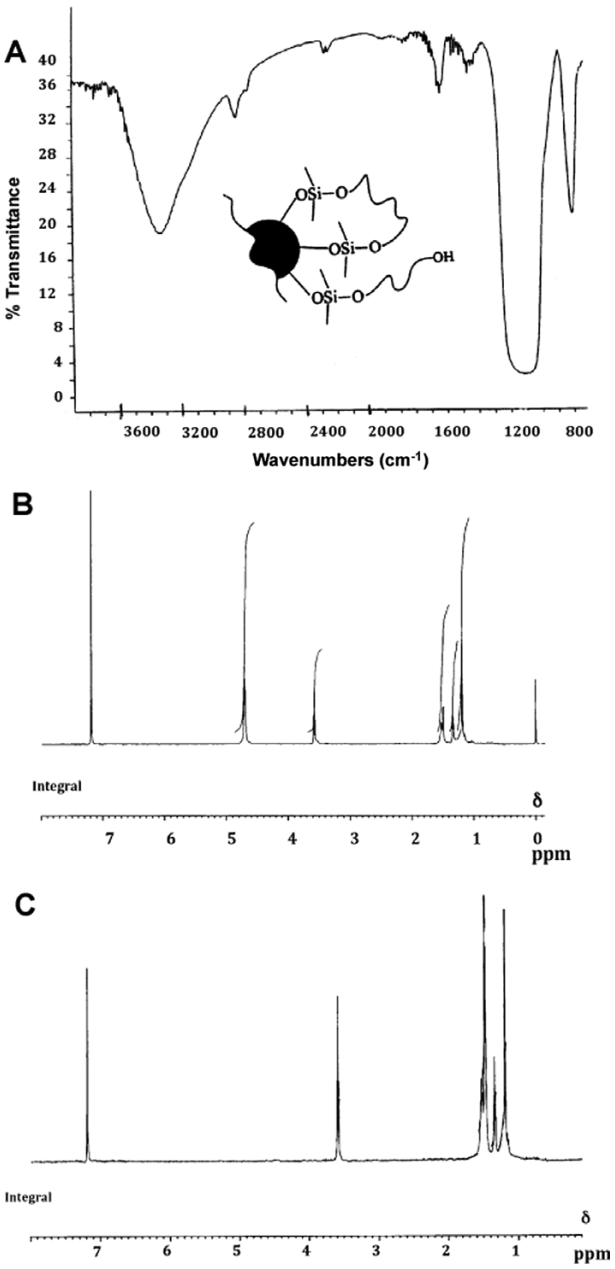

Figure 2. (A) IR spectrum of compound (**2**); (B) Proton NMR spectrum of compound (**2**); (C) Proton NMR spectrum of compound (**2**) after D_2O shake.

get rid of any unreacted hexane diol, and drying afforded compound (**2**) with pendant hydroxyl groups at the distal end. The presence of the hydroxyl groups was shown by the strong broad band at ~ 3428 cm^{-1} in IR, Figure 2(A).

Also, the hydroxyl-groups' proton peak in ^1H NMR, Figure 2(B), was assigned to the multiplet at 1.49-1.55 *via* an additional D_2O exchange experiment, Figure 2(C). GC-MS pyrolyis analysis for compound (**2**) showed a typical hexane diol pyrolysis cleavage pattern for the presence of alcohol with a straight-chain hydrocarbon backbone. The intensity

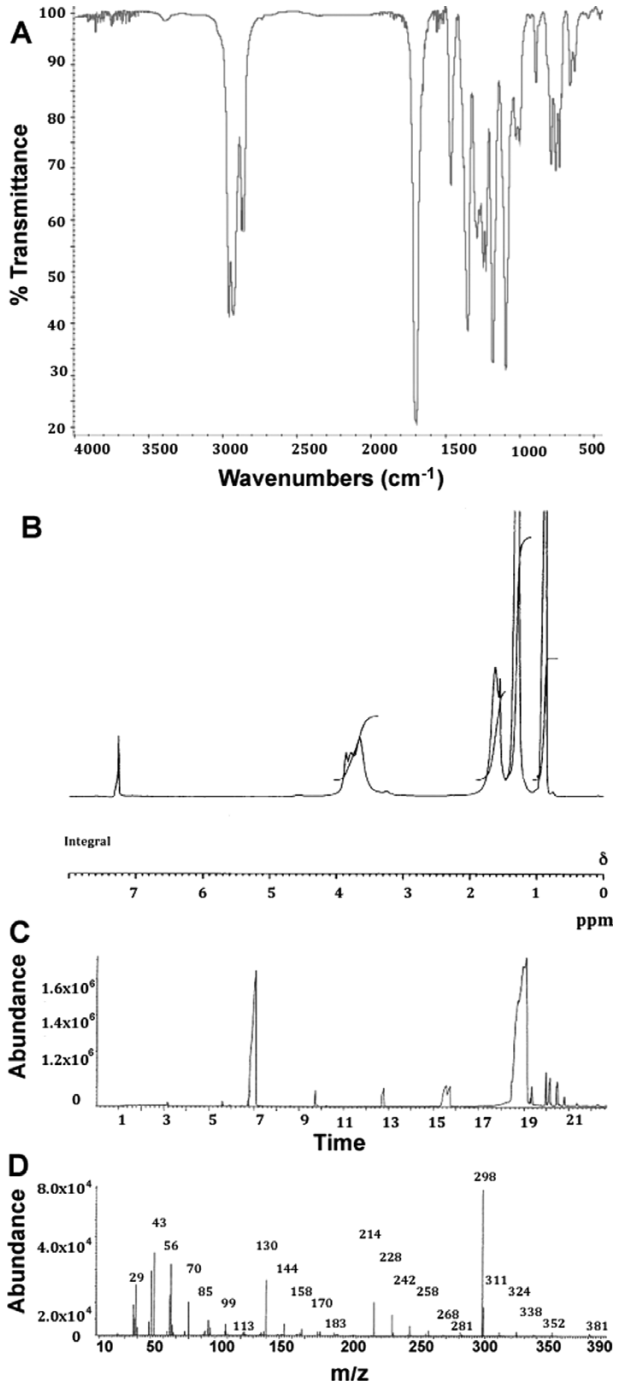

Figure 3. (A) FTIR spectrum of poly(*n*-hexyl isocyanate) grown silica surface, compounds (**4**) and (**5**); (B) Proton NMR spectrum of compounds (**4**) and (**5**); (C) Pyrolyis decomposition analysis of compound (**5**); (D) GC-MS mass spectrum of overloaded peak at 18.8 min.

of the molecular ion peak in the mass spectrum of primary alcohol is usually very low; in our system the molecular ion peak of the attached to the surface alcohol appears at m/e 117 which is a very low value. Moreover, the fragmentation pattern is in close accordance to that of an aliphatic primary alcohol with straight-chain hydrocarbons undergoing fragmentation by breaking carbon-carbon bonds, resulting in a homologous series of fragmentation products.

The hydroxyl groups of compound (**2**) were used to tether the $TiCl_4$ and thus to generate a substrate surface with an active transition metal catalyst, the titanium alkoxide, compound (**3**). This reaction was carried out under inert and dry conditions. This intermediate material (**3**) with the transition metal catalyst at the distal end is an extremely air, water, and temperature sensitive compound. Neat *n*-hexyl isocyanate monomer was added to (**3**) and polymerization was apparent from an increase in the viscosity of the reaction mixture yielding the compounds (**4**) and (**5**).

FTIR of the compounds (**4**) and (**5**), Figure 3(A), shows complete disappearance of the *n*-hexyl isocyanate monomer absorption at ~2250 cm^{-1}. Moreover, an attempt to polymerize *n*-hexyl isocyanate in the presence of (**2**), as a blank reaction, did not result in polymer formation, as expected. ^1H NMR of (**4**) and (**5**), Figure 3(B), shows 4 peaks. A multiplet at 3.9-3.4 is due to the protons at -CH_2 -N-. These protons would be deshielded due to the adjacent nitrogen. Another multiplet at 1.7-1.42 is due to protons at -CH_2 -CH_2- N-. Six protons absorb as a multiplet at 1.40-1.10. The methyl protons at -CH_3 -$(CH_2)_5$ -N absorb at 0.98-0.86 as a broad singlet.

GC-MS results for silica surface-grown poly(*n*-hexyl isocyanate), for both short and long chains (compounds (**4**) and (**5**)), Figure 3(C)-(D), show a simple fragmentation pattern. The mass of the molecular ion is 381 amu. This, on the other hand, due to the so-called 'nitrogen rule' (stating that a molecule with an odd number of nitrogen atoms will form a molecular ion with an odd mass) indicates that there is an odd number of nitrogen atoms in the polymer chains. Low molecular weight fragments, below 100 amu, started to appear just above 200 °C, which is correlated with the TGA thermogram of the material. The fragments appear to be due to consecutive cleavages of CH_2 fragments from the *n*-hexyl hydrocarbon pendant groups. The base fragmentation peak, with 298 amu, is due to the cleavage of the pendant *n*-hexyl group from the main isocyanate chain where the last one quickly traps two protons to form a positive radical ion. The *n*-hexyl fragment appears as 85 amu. With the loss of a CH_3 group, it creates a fragment with 70 amu. Further cleavage of the CH_2 group renders a fragment with 56 amu. Further fractionating yields fragments with 43 amu and 29 amu, respectively. The peak at 70 amu may also be, due to cyclization reactions that accompany the thermal decomposition with the yield of cyclopentane.

The length of the polymer chains grown from the silica surface was determined by GPC after cleaving off the polymer at the acid sensitive site *via* acid hydrolysis.[33-35] The polymer being stable to the acidic conditions remained unaffected by the cleavage procedure and had a molecular weight of ~64,000 g/mol and polydispersity of 1.3 for the long-chain, compound (**5**) and 21,500 g/mol and polydispersity 1.5 for

the short-chain polymer, compound (**4**), respectively. We have shown that we can achieve a good control over the polymer chain lengths with this "controlled-growth"-polymerization system by generating both long and short chain polymers of *n*-hexyl isocyante on the silica substrate. When the initiator to monomer ratio was small, the polymer chains formed were long, and when the initiator to monomer ratio was large, short polymer chains were obtained.

Pathway II was employed to demonstrate both control over the density of the polymer growth-sites and ability to form a more stable interface with polymer brushes attached *via* more stable O-Si-C bonds in comparison with the acid labile O-Si-O bonds of pathway I, Scheme II. In this pathway the dried silica was treated with a 9:1 molar ratio of trimethyl silyl chloride and 1-octenyl dimethyl chlorosilane to yield (**6**). The trimethyl silyl chloride was used as a non-reactive spacer group in order to control the spatial density of the polymer chains grown at the silica surface. Also, since the two silyl reagents are mono chloro-compounds, they would be reactive only at one end, and therefore no branching can take place. Compound (**6**) has a pendant olefinic functionality that was subsequently reacted to form hydroxyl groups at the distal end, compound (**7**).

The FTIR spectrum of compound (**6**), Figure 4(A), shows the C-H stretching absorptions belonging to the different hydrocarbon moieties. -CH_3 stretching peaks appear at 2960 cm^{-1} and 2870 cm^{-1}; -CH_2 stretching vibrations absorption appear at 2919 cm^{-1} and 2853 cm^{-1}. Since the saturated hydrocarbon chain is longer than four carbons, the stretching vibration due to -CH_2 absorption is pronounced. One can see that these absorption peaks are more intense than the absorption peaks from -CH_3. The sp^2 hybridized carbon-hydrogen stretching vibrations absorption appears as a shoulder above 3000 cm^{-1}.

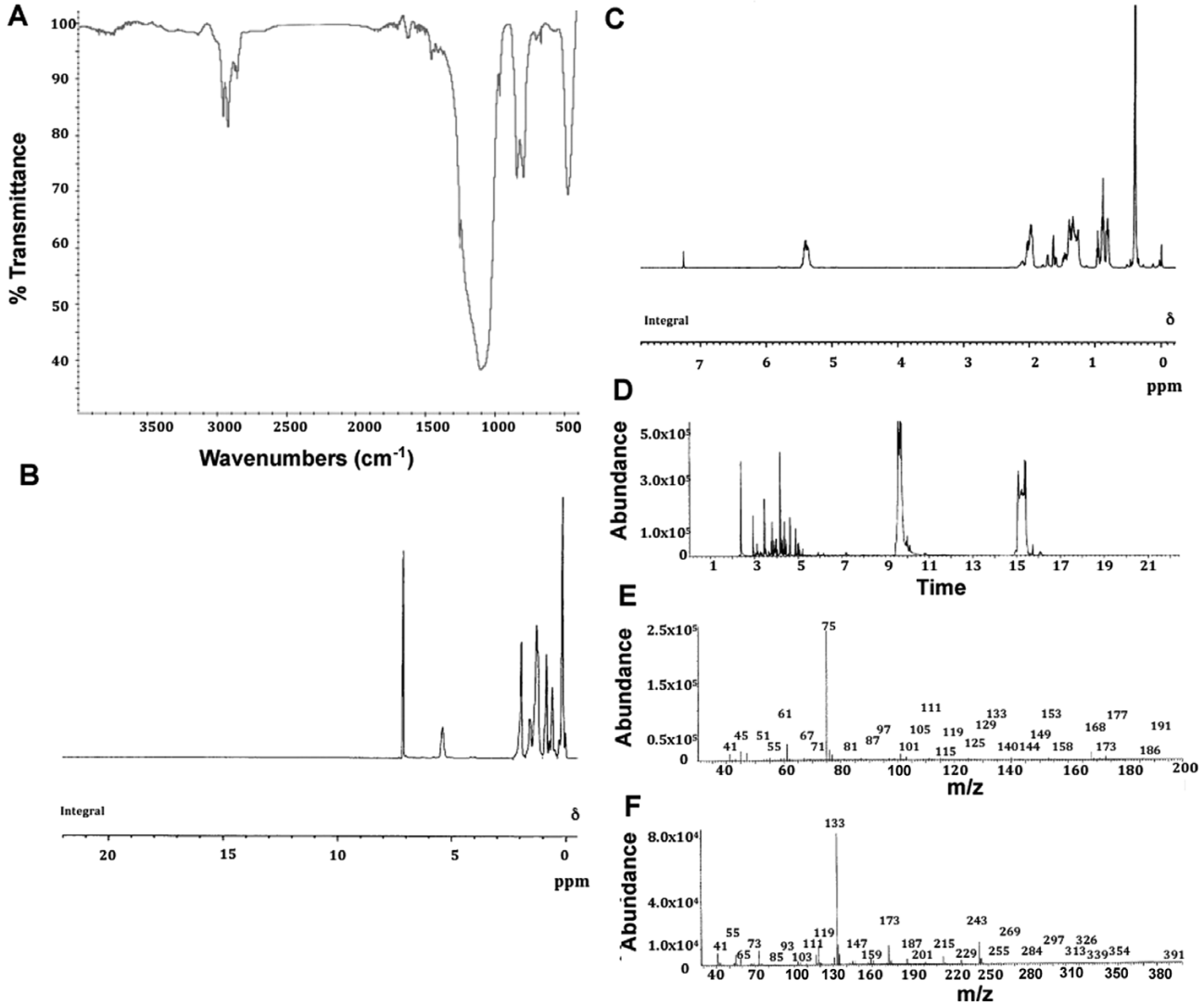

Figure 4. (A) FTIR spectrum of compound (**6**); (B) Proton NMR spectrum of compound (**6**); (C) Proton NMR spectrum of 7-octenyl dimethyl chlorosilane; (D) Pyrolysis decomposition analysis of compound (**6**); (E) GC-MS mass spectrum of overloaded peak at 9.4 min; (F) GC-MS mass spectrum of overloaded peak at 15-15.8 min.

Peaks for Si-O-Si asymmetric stretching vibrations, due to substrate, appear at 1100 cm^{-1}. The doublet at 840 cm^{-1} and 846 cm^{-1} is due to Si-O-Si in plane bending, whereas the peak at 472 cm^{-1} is due to Si-O-Si stretching vibrations absorption.

The proton NMR of compound (**6**), Figure 4(B), proves further that chlorotrimethylsilane and 7-octenyl dimethyl chlorosilane were indeed attached to the silica surface. The three vinylic protons appear at δ5.40. The two protons at the carbon next to the vinyl group appear at δ1.97. The Si-CH_2 protons appear at the δ0.95-0.62 region. The Si-CH_3 protons appear in the δ0.05-0.32 region. The rest of the CH_2 protons appear at the δ1.62-1.26 region. The integration ratios for the -HC=CH_2 protons versus -Si$(CH_3)_x$- has changed from 3:6 in the 7-octenyl dimethyl chlorosilane starting material to 3:15 in the product. For comparison see the proton NMR of the 7-octenyl dimethyl chlorosilane, Figure 4(C). In the NMR spectra of 7-octenyl dimethyl chlorosilane starting material, the three protons of the vinyl group appear at the δ5.41-5.38 region and the six protons from -Si$(CH_3)_2$- appear at the δ 0.41-0.39 region with proton ratio 3:6. The rest of the protons are distributed as follows: the two protons attached to the carbon next to the vinyl group appear at the δ1.99-1.96 region, the protons at Si-CH_2- appear at the δ0.95-0.79 region, and the rest of the protons are lying in the δ1.40-1.35 region. For compound (**6**), however, the ratio of -HC=CH_2 protons versus -Si(CH_3)- protons has changed to 3:15. The difference in the protons comes from the spacer. Moreover, in the NMR spectrum of the product we do not see the shift in -Si$(CH_3)_2$- protons due to the presence of chlorine attached to silica, another indication that the attachment to the surface took place (with elimination of HCl). The presence of a chlorine atom attached to silica causes a shift in the CH_3 protons that are also attached to the silica of δ0.4.

The GC-MS analysis of compound (**6**), Figure 4(D)-(F), taken in a 35 ºC to 500 ºC pyrolysis range with 15 ºC increments per minute and a 2 min hold at 35 ºC, show two distinct regions of fragmentation. The GC Phase, Figure 4(D), is indicating that the first fragmentation overload takes place at 9.4 min, which corresponds to a temperature just above 170 ºC and is possibly due to siloxane compounds (detailed in Figure 4(E)). The second fragmentation overload is at the 15-15.8 min range, *i.e.* around 260 ºC and is possibly due to disiloxane compounds (detailed in Figure 4(F)). The conducted pyrolysis analyses show extensive fragmentation of the hydrocarbon chains beginning at around 110 ºC. After cleavage of the 1-octenyl, 111 amu and trapping of a proton- 112 amu, an extensive homologous series fragmentation is observed. The hydrocarbon radical cation (after losing a π electron from the double bond) with 112 amu, fragments by releasing a CH_3 group. The product, a radical cation with 97 amu, disintegrates further to give the 83 amu fragment. By such consecutive CH_2 fragmentations, radical cations with atomic mass units of 70, 56, 42, and 43; and 70, 55, 41, 27 amu are observed, and this is a typical hydrocarbon fragmentation pattern. At a considerably lower temperature, around 9th minute and 180 ºC, the -Si$(CH_3)_2(CH_2)_6$CH=CH_2 radical cation fragment (168 amu) is observed, which undergoes further fragmentation with the typical hydrocarbon fragmentation pattern. Another very pronounced fragmentation radical around this temperature and as a consequence of further fragmentation is the -O-Si$(CH_3)_2$- fragment with 75 amu, as seen in Figure 4(E). The cleavage of the -Si$(CH_3)_3$ group, our spacer, with 73 amu occurs around the 15th min corresponding to temperature around 260 ºC, Figure 4(F). There is a very interesting feature at this temperature as if an instant formation of disiloxane takes place immediately after fragmentation so we see a fragment with 243 amu which may be the radical cation of $(CH_3)_2$HSi-O-Si$(CH_3)_2(CH_2)_3$CH=CH_2. The fragmentation of this disiloxane gives the $(CH_3)_2$HSi-O-Si$(CH_3)_2$- radical cation with 133 amu, as seen in Figure 4(F).

Hydroboration of compound (**6**) yielded product (**7**) with terminal hydroxyl functionalities. The presence of the hydroxyl groups can be shown by the IR spectrum with a broad band appearing at ~3400 cm^{-1}. FTIR of compound (**7**), Figure 5, with both peak-positioning and peak-characteristics fully supports the assigned structure. One can see all of the characteristic IR absorption peaks. Unlike the compound (**6**) spectrum, here one can see absorption due to -OH presence in the structure, the broad peak at around 3400 cm^{-1} and also the peak at 1630 cm^{-1} due to -OH bending vibrations absorption. Moreover, the shoulder-peak due to =C-H absorption above 3000 cm^{-1} has disappeared since all the vinyl has converted to alcohol during the hydroboration reaction. The presence of silica a core is confirmed by the Si-O-Si absorption peaks appearing at their usual wavenumber. Peaks for Si-O-Si asymmetric stretching vibrations appear at 1100 cm^{-1}. The peak around 840 cm^{-1} is due to Si-O-Si in plane bending, whereas the peak at 472 cm^{-1} is due to Si-O-Si stretching vibrations absorption.

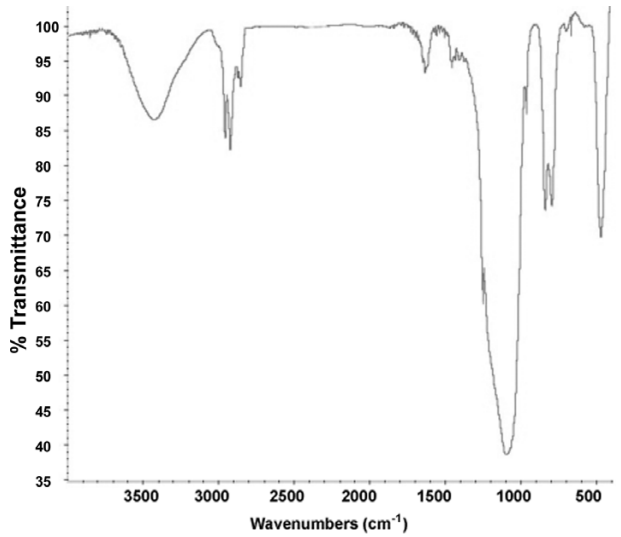

Figure 5. IR spectrum of compound (**7**).

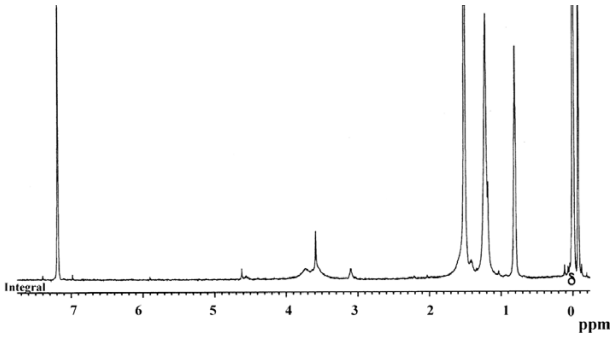

Figure 6. Proton NMR spectrum of compound (**9**).

The proton NMR of compound (**9**) shows that protons at the carbon α to the oxygen appear at δ 4.62. Protons α to the nitrogen appear as a broad peak at δ 3.59. Protons from the carbon β to nitrogen appear at δ 1.51. The protons at the third to the fifth carbon in the *n*-hexyl group appear at the δ 1.22-1.18 region. The protons at the sixth carbon of the *n*-hexyl group appear at δ 0.81. The -Si-CH_3- protons appear at the δ 0.00 to -0.070 region. The peak around δ 3.2 may be due to unreacted *n*-hexyl isocyanate monomer trapped between the brushes, Figure 6.

Percent-coverage of the silica surface with organic material was determined by thermogravimetric analyses (TGA), Figure 7. Thermograms comparison of dried silica, Figure 7(A)(a), with that of compound (**2**), Figure 7(A)(b), shows that the organic material covered silica, compound (**2**), undergoes almost 40% weight loss, whereas the unmodified silica shows almost no weight loss. The amount of the inorganic component in compound (**2**) is 60% with 40% organic component with maximum weight loss between 450 °C and 500 °C.

TGA results of compound (**6**), Figure 7(B), show that there are two main regions where substantial weight loss is observed. The first one is around 170 °C and the second one at around 260 °C with the latter having the highest weight loss. The pyrolysis GC-MS results (discussed earlier and characterizing the material-loss at specific temperatures) are supporting our results from the TGA study which are further indicating that the organic coverage is 41% of the total weight.

The thermogram of a poly(*n*-hexyl isocyanate) covered silica shows even more dramatic weight loss pattern, Figure 7(C). More than 96% of the material, which comprises the organic part, is lost. At above 300 °C, less than 5% of the original material is present, which is the inorganic part in the sample. The first weight loss appears just above 200 °C and is attributed to rapid degradation of hydrocarbon pendant chains. With elevation of the temperature, the isocyanate backbone degradation takes place.

We clearly see that the GC-MS and TGA study results are re-enforcing and complementing each other, as expected. The observed weight loss temperature and pattern is overlapping with the distinct fragmentation regions seen with the GC-MS mass spectra analyses that also identifies the released

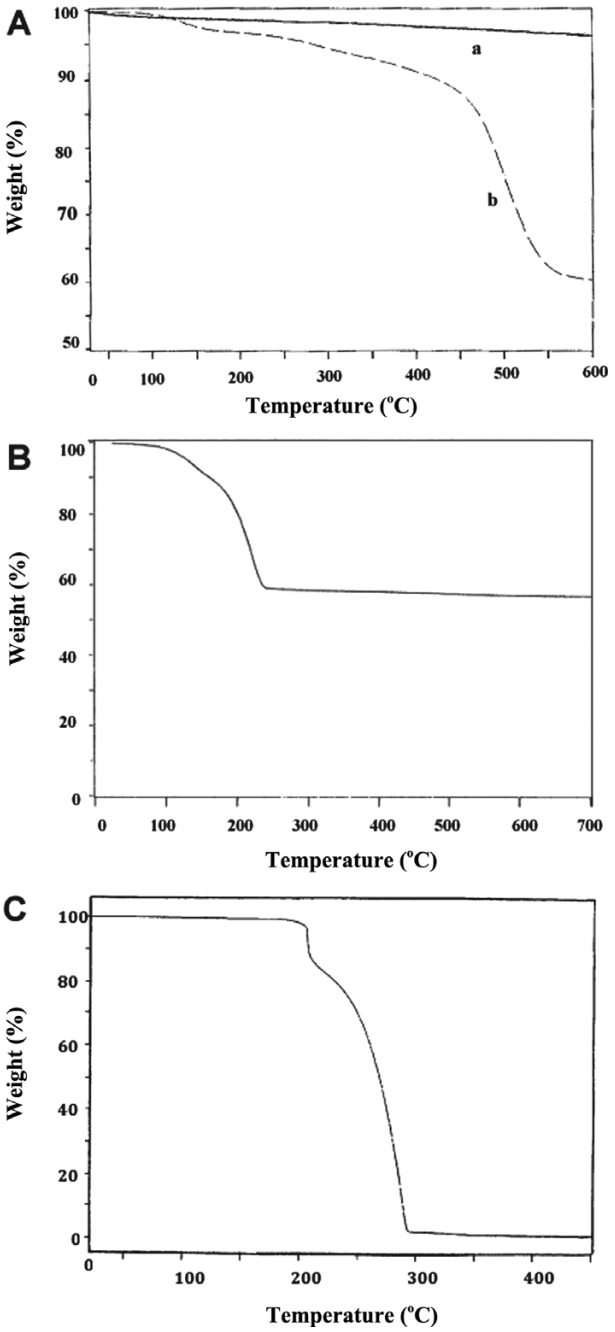

Figure 7. Thermogravimetric (TGA) analyses results of (A) (a) dried silica, (b) compound (**2**); (B) compound (**6**); (C) polymer grown silica.

fragments; with the spacer group fragmentation taking place at around 260 °C.

Interestingly, in our polymerization system the titanium catalyst showed to be quite robust and effective with polymerization process resuming after addition of fresh monomer with mainly chain growth propagation process that are also some of the attributes of the "living polymerization" systems.[36-38] Moreover, the polymerization process was observed to be fac-

ile and subsequent work-ups easy to handle and scale up.

Considering that our silica surface has 3.5 to 4.5 OH groups/nm^2, as identified by Liu and Maciel[25] as well as the manufacturer, which is equivalent to 3.5×10^{18} to 4.5×10^{18} OH groups/m^2, according to this, the number of OH sites can be calculated as:

$$\begin{aligned}\#\text{ of OH sites} &= (200\pm50\ \text{m}^2/\text{g})(3.5\times10^{18}\text{-}4.5\times10^{18}\ \text{OH groups/m}^2)\\ &= 7\times10^{20}\text{-}9\times10^{20}\ \text{OH sites/g}\\ &= 1.16\times10^{-3}\text{-}1.5\times10^{-3}\ \text{mol of sites/g}\end{aligned}$$

which effectively is the active molar concentration of the surface silanols, *i.e*. 1.16 to 1.5 mmol/g of silanol groups is potentially available for catalyst sequestering. If each of these surface-OH sites becomes a polymer chain with a molecular weight of 64,000 or 21,500 g/mol, respectively, the percent of organic component in the inorganic-core polymeric nanocomposite should be 98.67% or 96.16%, respectively, which is in good agreement with our TGA results.

Conclusions

We have shown that surface-initiated polymerization of polymer brushes of *n*-hexyl isocyanate with titanium catalyst is a viable technique to generate polymeric nanocomposites with stable and controlled surface functionalization. Due to the nature of the polymerization mechanism and the fact that this is a living polymerization we were able to attain NP surface bound polymer with various molecular weights and narrow polydispersity. We were able to demonstrate that both control over the polymer growth-sites densities and ability to form a more stable interface with polymer brushes attached *via* more stable O-Si-C bonds in comparison with the acid labile O-Si-O bonds are attainable. Our research opens up new possibilities to create responsive "smart" surfaces with high density of surface grown polymer.

Acknowledgments. MRH was supported by US NIH grant R01AI050875.

References

(1) M. Manca, A. Cannavale, L. De Marco, A. S. Arico, R. Cingolani, and G. Gigli, *Langmuir : the ACS Journal of Surfaces and Colloids*, **25**, 6357 (2009).
(2) J. Bravo, L. Zhai, Z. Wu, R. E. Cohen, and M. F. Rubner, *Langmuir : the ACS Journal of Surfaces and Colloids*, **23**, 7293 (2007).
(3) J. F. Chen, H. M. Ding, J. X. Wang, and L. Shao, *Biomaterials*, **25**, 723 (2004).
(4) A. Burns, H. Ow, and U. Wiesner, *Chem. Soc. Rev.*, **35**, 1028 (2006).
(5) H. H. Yang, S. Q. Zhang, X. L. Chen, Z. X. Zhuang, J. G. Xu, and X. R. Wang, *Analytical Chemistry*, **76**, 1316 (2004).
(6) E. Katz and I. Willner, *Angew. Chem.*, **43**, 6042 (2004).
(7) B. Radhakrishnan, R. Ranjan, and W. J. S. M. Brittain, *Soft Matter*, **2**, 386 (2006).
(8) H. Zou, S. Wu, and J. Shen, *Chem. Rev.*, **108**, 3893 (2008).
(9) Z. Chen, Z. M. Cui, C. Y. Cao, W. D. He, L. Jiang, and W. G. Song, *Langmuir : the ACS Journal of Surfaces and Colloids*, **28**, 13452 (2012).
(10) S. Edmondson, V. L. Osborne, and W. T. Huck, *Chem. Soc. Rev.*, **33**, 14 (2004).
(11) O. Pruker and J. Ruhe, *Mater. Res. Soc. Symp. Proc.*, **304**, 1675 (1993).
(12) T. E. Patten and B. M. Novak, *Macromolecules*, **26**, 436.
(13) R. Cook, R. D. Johnson, C. G. Wade, D. J. O'Leary, B. Munoz, and M. M. Green, *Macromolecules*, **34**, 3454 (1990).
(14) P. L. Dubin and J. M. Principi, *Macromolecules*, **22**, 1891 (1989).
(15) L. S. Hegedus, *Transition Metals in the Synthesis of Complex Organic Molecules*, University Science Books, New York, 1994.
(16) U. Shmueli, W. Traub, and K. Rosenheck, *J. Polym. Sci.*, *Part B: Polym. Phys.*, **7**, 515 (1969).
(17) S. Lifson, C. Felder, and M. M. Green, *Macromolecules*, **25**, 4142 (1992).
(18) E. Bianco, A. Ciferri, G. Conio, and W. R. Krigbaum, *Polymer*, **28**, 813 (1987).
(19) T. Itou and A. Teramoto, *Macromolecules*, **21**, 2225 (1988).
(20) M. M. Green, C. Andreola, B. Munuz, M. P. Rridy, and K. Zero, *J. Am. Chem. Soc.*, **110**, 4063 (1988).
(21) M. M. Green, C. Khatri, and N. C. Peterson, *J. Am. Chem. Soc.*, **115**, 4941 (1993).
(22) L. D. Belyakova, O. M. Dzhigit, A. V. Kiselev, and R. J., *Phys. Chem. Engl. Trans.*, **33**, 551 (1959).
(23) H. P. Boehm, *Angew. Chem.*, **5**, 533 (1966).
(24) M. L. Hair, *Infrared Spectroscopy in Surface Chemistry*, Dekker, New York, 1967.
(25) C. C. Liu and G. E. Maciel, *J. Am. Chem. Soc.*, **118**, 5103 (1996).
(26) I.-S. Chuang and G. E. Maciel, *J. Am. Chem. Soc.*, **118**, 401 (1996).
(27) A. Vrij and A. P. Philipse, *J. Colloid Interface Sci.*, **128**, 121 (1989).
(28) W. Stober, A. Fink, and E. Bohn, *J Colloid Interface Sci.*, **26**, 62 (1968).
(29) E. F. Vansant, P. Voort, and K. C. Vrancken, *Characterization and Chemical Modification of the Silica Surface*, Elsevier, New York, 1994.
(30) R. K. Iler, *The Chemistry of Silica: Solubility, Polymerization, Colloid and Surface Properties, and Biochemistry*, Wiley, New York, 1979.
(31) J. Wong and C. A. Angell, *Glass Structure by Spectroscopy*, Marcell Dekker, New York, 1976.
(32) *Porous Silicon*, World Scientific, Singapore, 1994.
(33) E. J. Corey and A. Venkateswarlu, *J. Am. Chem. Soc.*, **94**, 6190 (1972).
(34) E. J. Corey and B. B. Snider, *J. Am. Chem. Soc.*, **94**, 2549 (1972).
(35) E. Nakamura and I. Kuwajima, *J. Am. Chem. Soc.*, **97**, 3257 (1975).
(36) O. W. Webster, *Science*, **251**, 887 (1991).
(37) R. P. Quirk and B. Lee, *Polym. Int.*, **27**, 359 (1992).
(38) J. Khadem, A. A. Veloso, Jr., F. Tolentino, T. Hasan, and M. R. Hamblin, *Invest Ophthalmol Vis Sci.*, **40**, 3132 (1999).